WRC RESEARCH REPORT No. 155

MEASUREMENTS IN MERGING FLOW

by

W. Hall C. Maxwell

and

Arni Snorrason

Department of Civil Engineering

University of Illinois at Urbana-Champaign

Urbana, Illinois 61801

FINAL REPORT

Project No. A-103-ILL

This project was partially supported by the U. S. Department of the Interior in accordance with Title I of the Water Research and Development Act of 1978, P.L. 95-467, Agreement No. 14-34-0001-0115.

UNIVERSITY OF ILLINOIS
WATER RESOURCES CENTER
2535 Hydrosystems Laboratory
Urbana, Illinois 61801

January 1981

ABSTRACT

Previous measurements of the velocity field in the vicinity of two intersecting submerged turbulent jets provided evidence that, contrary to the usual assumptions, intersecting flows may not necessarily be combined using vector addition of velocities or momentum flux densities.

To gather additional experimental evidence on the details of the velocity field near the intersection of two submerged turbulent jets, this study measured time average velocity magnitudes and directions of two perpendicular intersecting axisymmetric submerged turbulent incompressible air jets of approximately equal strength. Because of the need to detect reverse flows, a three-dimensional pitot-type probe was used. This could sense yaw and pitch angles as well as velocity magnitudes. Two sets of measurements were taken. The more detailed set was confined to the plane of the nozzles, the less detailed set obtained cross-sectional data at four stations, three of these being in the observed reverse flow.

The data show that the reverse flow spreads much more rapidly perpendicular to the nozzle plane than in the nozzle plane, whereas the forward flow is fairly symmetric. Similarity profiles were found in both the forward and reverse flows. In the forward flow the distribution was essentially Gaussian. This was also true in the backward flow in the direction normal to the plane of the nozzles. In the plane of the nozzles the backward flow profiles were close to semi-elliptical or semi-circular, depending on the scales for plotting.

Maxwell, W. Hall C., and Arni Snorrason
MEASUREMENTS IN MERGING FLOW
Final report to the Office of Water Research and Technology,
Department of Interior Project A-103-ILL, January 1981.

KEYWORDS: *Diffusion-flow/flow characteristics/*flow profiles/fluid mechanics/*jets/*mixing

TABLE OF CONTENTS

LIST OF TABLES

LIST OF FIGURES

LIST OF SYMBOLS

A	incoming jet nozzle, see Fig. 1
A_o	outlet area (per unit length for slot)
B	incoming jet nozzle, see Fig. 1
b_y	half width of velocity profile in xy plane
b_z	half width of velocity profile in xz plane
C	spreading coefficient
j	= 0 for plane symmetry, = 1 for axial symmetry
P_1	total pressure
P_2, P_3	pressures sensed by lateral ports
P_{23}	$= P_2 - P_3$
P_4, P_5	pressures sensed by upper and lower ports
P_{45}	$= P_4 - P_5$
P_s	true static pressure
P_t	true total pressure
u	time average velocity in the x direction, or velocity magnitude
u_o	average velocity at outlet
u_a	average velocity at nozzle A outlet
u_b	average velocity at nozzle B outlet
u_m	maximum or centerline velocity
x, y, z	orthogonal co-ordinate axes
β	angle of pitch
Δy	y deviation from location of maximum velocity
Δz	z deviation from location of maximum velocity
θ	angle of yaw
σ_y	standard deviation of velocity profile in xy plane
σ_z	standard deviation of velocity profile in xz plane

2. VELOCITY DISTRIBUTION IN A SINGLE JET

The velocity distribution in a submerged turbulent jet had been considered by many investigators to be adequately described by a normal distribution. For both plane-symmetric and axisymmetric jets, the velocity distribution may be described by the following equation:

$$\frac{u}{u_o} = \frac{A_o^{1/2}}{[\pi^{1/2} C\, x]^{(j+1)/2}} \exp\,[0.5\ (y/(Cx))^2] \qquad (1)$$

in which u = time average velocity in the axial, x, direction; u_o = average velocity at the outlet; A_o = outlet area (per unit length for plane-symmetry); C = spreading coefficient; y = axis normal to x (radial axis for axial symmetry); j = 0 for plane symmetry, and j = 1 for axial symmetry.

Different investigators have obtained different experimental values for C, the spreading coefficient, in the case of both the plane-symmetric jet and the axisymmetric jet. These results are dealt with in detail in the following section.

2.2 Spreading Coefficients for Plane- and Axi-Symmetric Jets.

Table 1 summarizes spreading coefficients measured by a number of investigators for two-dimensional turbulent jets. The information has been collected from Refs. 1, 10, 27 and 33. Where possible the original source of data has been listed in the References. The table reflects the fact that three different sources (1, 26, 33) gave three different values of C from fitting Förthmann's data. Round-off error in converting from the notation of Refs. 1, 27 and 33 to the present notation may account for part

TABLE 1. Measured Two-dimensional Spreading Coefficients

Experimenter	Year	Axial C	Lateral C
Förthmann	1934	0.098	0.082,0.084,0.086
Reichardt	1942	-	0.095
van der Hegge Zijnen	1949	0.114	0.084
Albertson et al.	1950	0.109	0.109
Reichardt	1951	-	0.098
Miller & Comings	1957	0.093	0.082
van der Hegge Zijnen	1958	0.092	0.082
Nakaguchi	1961	0.107	0.090
Olson	1962	0.100	0.090
Bradbury	1963	0.100	0.068
Heskestad	1963	0.098(?)	0.090
Knystautas	1964	0.097	0.090
			0.088
Gartshore	1965	0.092	0.087
Heskestad	1965	-	0.093
Goldschmidt & Eskinazi	1966	-	0.084
Flora & Goldschmidt	1969	-	0.093
Mih & Hoopes	1972	-	0.099
Jenkins & Goldschmidt	1973	-	0.075
Kotsovinos	1975	-	0.093
			0.074
Average ± st. dev.		0.100±0.007	0.088±0.009

Selected Average by:	Year	Average Axial C	Average Lateral C
Newman	1961	-	0.088±2%
Abraham	1963	0.101	0.100
Fischer et al.	1979	0.097±0.003	0.082±0.001

of the differences. The table shows values obtained by fitting the data for decay of the maximum velocity along the axis and values obtained by fitting the distributions normal to the axis. Depending on one's objectives, one may obtain a "best" fit to either of these data sets or, by compromising slightly on the goodness of fit in both cases, select a single spreading coefficient which applies reasonably well to both cases e. g. the result obtained by Albertson et al. (2). This may then be used with Eq. 1. A further opportunity for some compromise arises in the selection of a zero correction or slight shift in the origin of the co-ordinate system from the physical location of the slot outlet.

Newman (33) concluded that variations in lateral spreading coefficients evident from an examination of the work of earlier investigators was apparently largely due to end effects. Earlier measurements were made with low aspect-ratio slots, and insufficient care was taken to provide fairings on the end plates or to make them adequately large. This leads to values of spreading coefficient which are too low. He postulated that vortices forming at the edge of the end plates induce spanwise flows which usually thin the shear flow. Since this problem does not arise for axisymmetric jets, variations in measurements of their rate of growth are much less. Based on a neglect of doubtful measurements Newman recommended a lateral spreading coefficient of 0.088 ± 2%.

Albertson et al. (2) stated "....close agreement in the limited zone of establishment is considered less significant than evaluation of both zones (as in the two-dimensional case) in terms of the same coefficient...."

Abraham (1) selected average values of 0.101 for axial decay and 0.100 for lateral spreading at large distances from the outlet in his

TABLE 2. Measured Axi-symmetrical Spreading Coefficients

Experimenter	Year	Axial C	Lateral C
Trüpel	1915	-	0.079
Betz	1923	-	0.075
Ruden	1933	0.078	0.073, 0.076
Reichardt	1942	-	0.072
Corrsin	1943	-	0.071
Corrsin and Uberoi	1949	0.076	0.072
Hinze and v.d. Hegge Zijnen	1949	0.078	0.071
Keagy and Weller	1949	-	0.075
		-	0.070
Keagy, Weller, Reed & Reid	1949	0.086	0.075
Albertson, Dai, Jensen & Rouse	1950	0.081	0.081
Becher	1950	0.077	-
Corrsin and Uberoi	1950	-	0.081, 0.092
Reichardt	1951	-	0.072
Taylor, Grimmett, & Comings	1951	0.076	0.074
Alexander, Baron & Comings	1953	0.075	0.075
Forstall and Gaylord	1955	0.078	0.076, 0.078
Poreh and Cermak	1959	0.065	0.071
Ricou and Spalding	1961	-	0.081
Rosenweig, Hottel & Williams	1961	-	0.076
Johannesen	1962	-	0.073
Kizer	1963	-	0.070
Wilson and Danckwerts	1964	-	0.085, 0.081
Uberoi and Garby	1967	-	0.064, 0.071
Average ± st. dev.		0.077±0.005	0.075±0.006

Selected Average by:	Year	Average Axial C	Average Lateral C
Newman	1961	-	0.072
Abraham	1963	0.081	0.081
Fischer et al.	1979	0.081±0.001	0.076±0.002

study. He remarked that the data of Albertson et al. indicate that the lateral spreading coefficient actually tends to increase with increasing distance from the outlet. He indicated that other experimental work showed similar trends, which agrees with observations that lateral distributions of turbulent stresses in axisymmetric jets (7) and in two-dimensional jets (31) do not exhibit similarity for distance less than 40 diameters or 40 slot heights downstream from the outlet.

Kotsovinos (27) also advanced the hypothesis that the basic reason for variations in spreading coefficients for plane turbulent jets is that growth is not exactly linear on a large scale. Data from several sources indicated that the jet width is a 'weak' non-linear function of x. No explanation was advanced for the observed behavior.

Fischer et al. (10) summarized values of lateral and axial spreading coefficients but did not detail the original sources incorporated in the averages.

Clearly, then, there is no consensus on "correct" values for either axial or lateral coefficients for two-dimensional jets.

Table 2 summarizes axial and lateral spreading coefficients for axisymmetrical jets, again taken from Refs. 1, 10, and 33. In some cases where two values are listed for the same test, e.g. Ruden, 1933, the table reflects the fact that Abraham (1) and Fischer et al. (10) obtained different values of C from fitting the data. The difference again also includes effects of round-off error when converting from the notation used by Abraham and by Fischer et al. to the notation used herein. Table 2 illustrates that there is also no consensus on "correct" values of axial or lateral coefficients for axi-symmetrical jets.

3. EXPERIMENTAL MEASUREMENTS IN CROSSING FLOWS

3.1 Purpose and Scope

Measurements of velocity time average magnitude and direction were aimed at detailed mapping of the velocity field in the vicinity of two intersecting incompressible air jet flows. In particular, there was an interest in the three-dimensional character of the resulting jet-like flows. Figure 1 shows a definition sketch of the various elements of the flow pattern. Measurements were made holding α at 90° and the quotient u_a/u_b in the narrow range 1.015 ± 0.001. The discharge through tubes A and B was held constant by monitoring the pressure at and across the orifice meters in their supply lines (Fig. 2). The co-ordinate system was aligned with the x-axis approximately parallel to CD, the axis of maximum velocity for the resultant flow, and the y-axis parallel to a line through the tube outlets.

3.2 Experimental Apparatus

The apparatus used to study the velocity distribution in the flow field created by two crossing air jets is illustrated in Fig. 2. Two identical 3/16 in. (0.475 cm) internal diameter copper tubes were used as nozzles and were mounted perpendicular to each other on a horizontal board. Each copper tube was connected to a 1 1/2 in. (3.8 cm) diameter pipe by means of tygon tubes. In order to maintain and monitor constant pressure, a pressure regulator and gauge were installed in the air supply upstream from the 1 1/2-in. pipe. A differential water manometer was used to measure the pressure drop across the orifice. The pressure on the upstream side of the plate was measured using a mercury manometer. The horizontal board was levelled on a table top, and a probe traversing mechanism

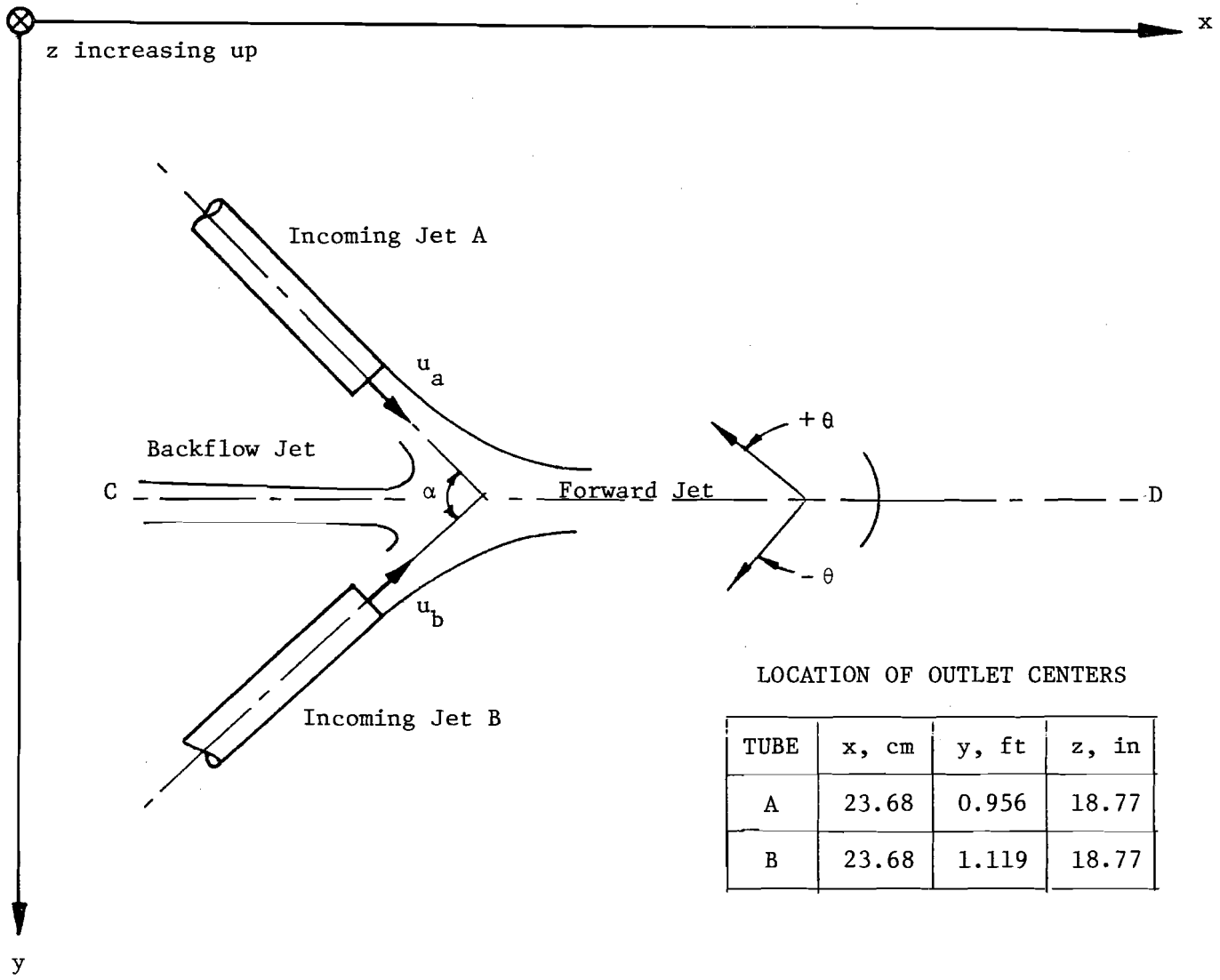

LOCATION OF OUTLET CENTERS

TUBE	x, cm	y, ft	z, in
A	23.68	0.956	18.77
B	23.68	1.119	18.77

Fig. 1 Definition sketch

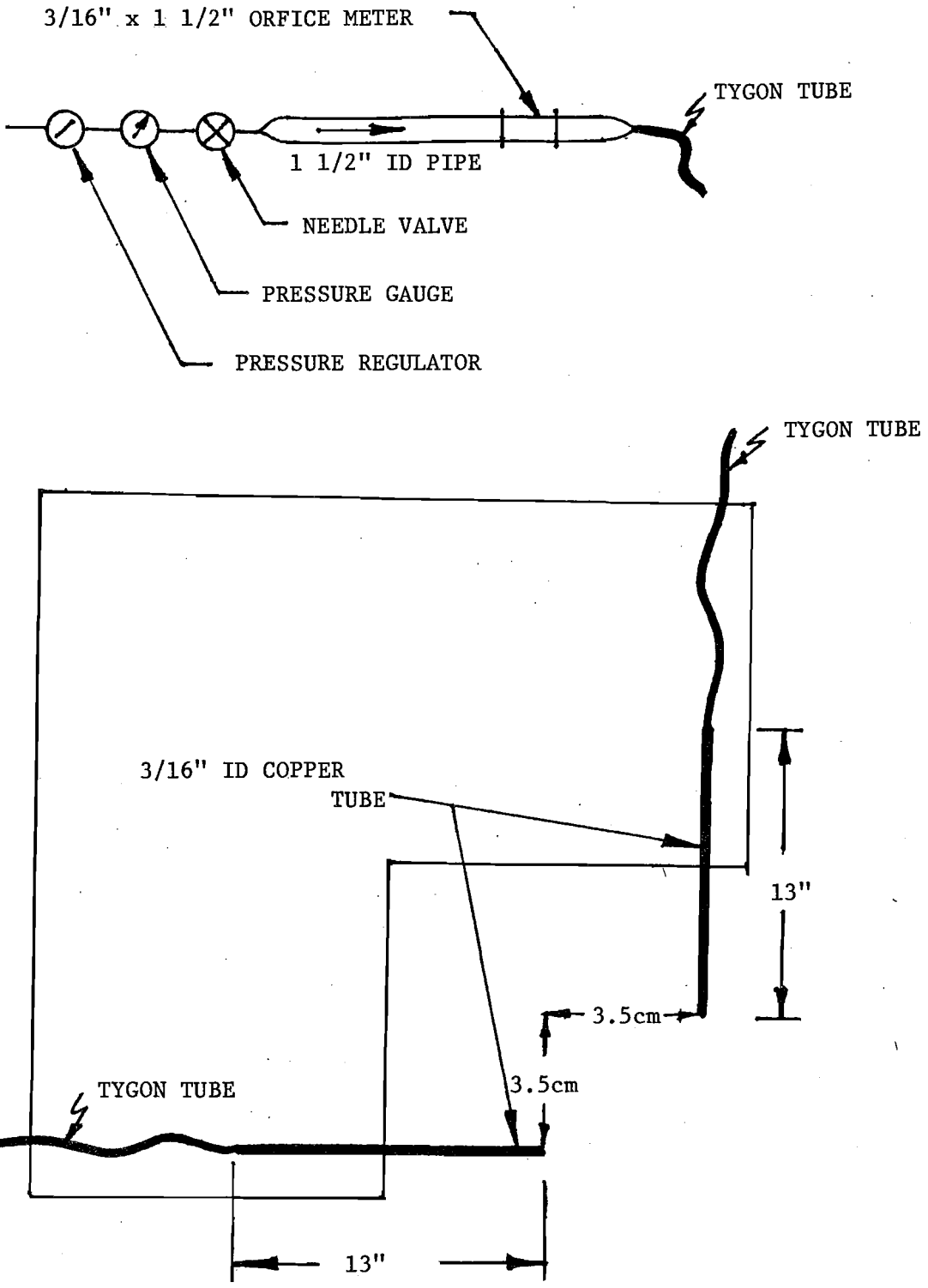

Fig. 2 - Schematic representation of crossing air jet apparatus

was mounted on a rigid framework independently mounted on the floor.

Time average velocity magnitudes and directions were measured using a United Sensor and Control Corporation Type DC three-dimensional directional probe. This had a sensing head diameter of 1/8-in. (0.318 cm) and a length of 36-in. (91.4 cm). It was mounted on a United Sensor and Control Corporation manual traverse unit. This has both a linear vernier traversing scale for distance readings and a rotary vernier scale for angle of yaw readings. The readings precision on the linear scale was 0.01 in. (0.025 cm) and 0.1 degrees on the angular vernier scale.

The manual traverse unit was mounted on a sturdy horizontal carriage running on a larger horizontal carriage. This in turn ran perpendicularly on horizontal rails incorporated in a heavy steel frame and was moved using a point gage set horizontally. The velocity probe, thus mounted, could be moved in three mutually orthogonal directions and rotated without altering the location of the sensing head. Co-ordinates were recorded to 0.01 in. (0.025 cm), 0.001 ft (0.030 cm) and 0.1 cm (0.039 in.), using the manual traverse, point gage reading and main carriage location scales respectively.

The three-dimensional directional probe measures the yaw and pitch angle of the velocity vector as well as total and static pressures. Five sensing ports are located on the tip of the probe. The centrally located port senses the total pressure P_1. The two lateral ports sense pressures P_2 and P_3. The probe is rotated using the manual traverse unit until $P_2 = P_3$ as indicated on a differential manometer. The vernier on the circular scale of the manual traverse unit then indicates the yaw angle.

With the probe aligned along the direction for which $P_{23} = P_2 - P_3 = 0$ the differential pressure $P_{45} = P_4 - P_5$ sensed by the two ports above and below the total pressure port is read on a differential manometer. The calibration curve for the probe can then be used to determine the angle of pitch. This is a function of P_{45}/P_{12}, in which $P_{12} = P_1 - 1/2\ (P_2 + P_3)$. For any particular pitch angle, β, the calibration curve of $(P_t - P_s)/P_{12}$ may be used to determine the velocity. P_t = true total pressure and P_s = true static pressure. The fluid velocity is

$$u = [2(P_t - P_s)/\rho]^{1/2} \qquad (2)$$

The differential manometers fluid was Meriam 827 Red Oil which has a specific gravity of 0.827. The P_{12} manometer was tilted at 45°; the P_{23} and P_{45} manometers were tilted at 20.5°. For data reduction the calibration curve for pitch angle was approximated by two linear functions, one for pitch angles in the range ± 10° with maximum error of 1°, the other for ± 40° with maximum error of ± 2.5°. The pitch angle measurements were unreliable when velocities, and hence P_{12}, were low. A lower limit of 0.8 lbs per square foot was therefore set on measurements of P_{12}. A good approximation to the calibration curve for pitch angles in the range ± 10° is the constant value 0.87 for $(P_t - P_s)/P_{12}$. Since the vast majority of reliable readings fell within this range this constant value was used for data reduction.

3.3 Experimental Measurements

For each measurement set the atmospheric temperature and pressure were recorded. For the mapping of the velocity vector field in the plane of the nozzles (z = 18.77 cm) traverses were made at constant values of x, with y being varied. The z-setting was found by traversing the pitot until

maximum velocity was found. Traverses were repeated at x intervals ranging from 0.1 cm up to 0.5 cm, so as to cover the incoming jets, the forward jet and the back flow jet. The values of P_{12}, P_t, yaw angle and P_{45}, as well as the coordinates (x, y, z) of the probe tip were recorded at each point of the traverse. In the zone near the stagnation point, velocities in the back flow jet were very small and there was interference between the probe and the incoming jets. The back flow jet measurements were therefore conducted with constant yaw angle. The yaw angle was set by moving back into a region of higher velocity back flow. The applicability of holding the yaw angle constant in the entire back flow region was checked from time to time where the back flow velocity was sufficiently high to permit it, and proved to be adequate. Similar difficulties were found near the edges of the incoming jets adjacent to the backflow jet and were again resolved by setting the yaw angle to its value in the adjacent region of higher incoming velocity. In all other portions of the flow field the pitot was set at the yaw angle determined by $P_{23} = 0$.

Because adjustment of the yaw angle was very time-consuming and considerably more data points had to be collected for mapping of the cross-sectional velocity field, the yaw angle was set at a constant value determined in the region of maximum velocity for the forward jet. Traverses were made at constant yaw angle and constant x. For each cross-section traverses were made in the y direction for various values of z. Three cross sections were measured for the back flow jet and one for the forward jet. The values of P_{12}, P_t, P_{45} and x, y and z were recorded for each point while holding the yaw angle constant.

3.4 Data Reduction

Computer programs were developed to analyze and present the data. Three sets of programs were utilized: one for handling raw data; one for graphical presentation of the velocity vector field in the plane of the nozzles; and one for graphical presentation of the cross-sectional data.

The program for handling of raw data calculated pitch angles and velocity pressure coefficients by linear interpolation of the calibration curves for the probe. The outlet average velocities were calculated using the calibrations for the orifice meters used in the supply lines to determine the air discharge.

The second program non-dimensionalized the raw data and plotted the variation of the velocity, yaw angle, θ, and pitch angle, β, for each traverse. A subroutine was used to plot the vector field, showing the angle of yaw and the length of the velocity vector. The interface between the back flow jet and the incoming jets A and B was not well defined. The most probable explanation is that the incoming jets interfere with the pitot tube when the backflow jet is measured and the backflow jet interferes with the pitot tube when the incoming jets are measured. Two sets of plots were prepared, one giving the forward velocities readings priority, the other giving priority to the backward velocities. The zone where the plots disagree indicates the region of interference.

The program for the cross-sectional data was used to plot contour or isovelocity plots and to illustrate three dimensional surfaces viewed from different vantage points.

3.5 Experimental Data

Figure 3 shows a plot of the velocity vector field in the plane of the jet nozzles. This plot is a composite of the plots described in the last section. The plot giving backward velocities priority was laid over the plot giving the forward velocities priority. The region of disagreement between these two is hatched in Figure 3, which is basically the backward priority plot. There may be some correlation between the fact that more conflict is observed on one side of the flow pattern and the fact that the probe always progressed into the flow field from that side. Note also that the linear scale is indicated at the top of the figure. Some of the measurements were taken at a later time than others,and it was noted that the maxima of the later and earlier profiles did not quite line up. This was attributed to slop in the carriage rail system, and an indication of its order of magnitude is noted on the figure. This problem did not present itself during any continuous set of measurements and only became evident near the end of the experimental program when some measurements were made to fill in gaps in the vector field plot. It would appear to be reasonable to shift the profiles to align the maxima; however the data are presented as recorded. Figure 3 is useful in assessing the overall character of the flow. However the detailed traverses upon which it is based are more useful in analysing the existence or not of similarity profiles within the flow and their detailed character. Two cross-sectional locations are flagged on Fig. 3 at x values of 25.4 cm and 26.0 cm. The detailed traverses for these two locations are presented in Figs. 4 and 5. Figure 4 shows the variation of velocity magnitude, yaw

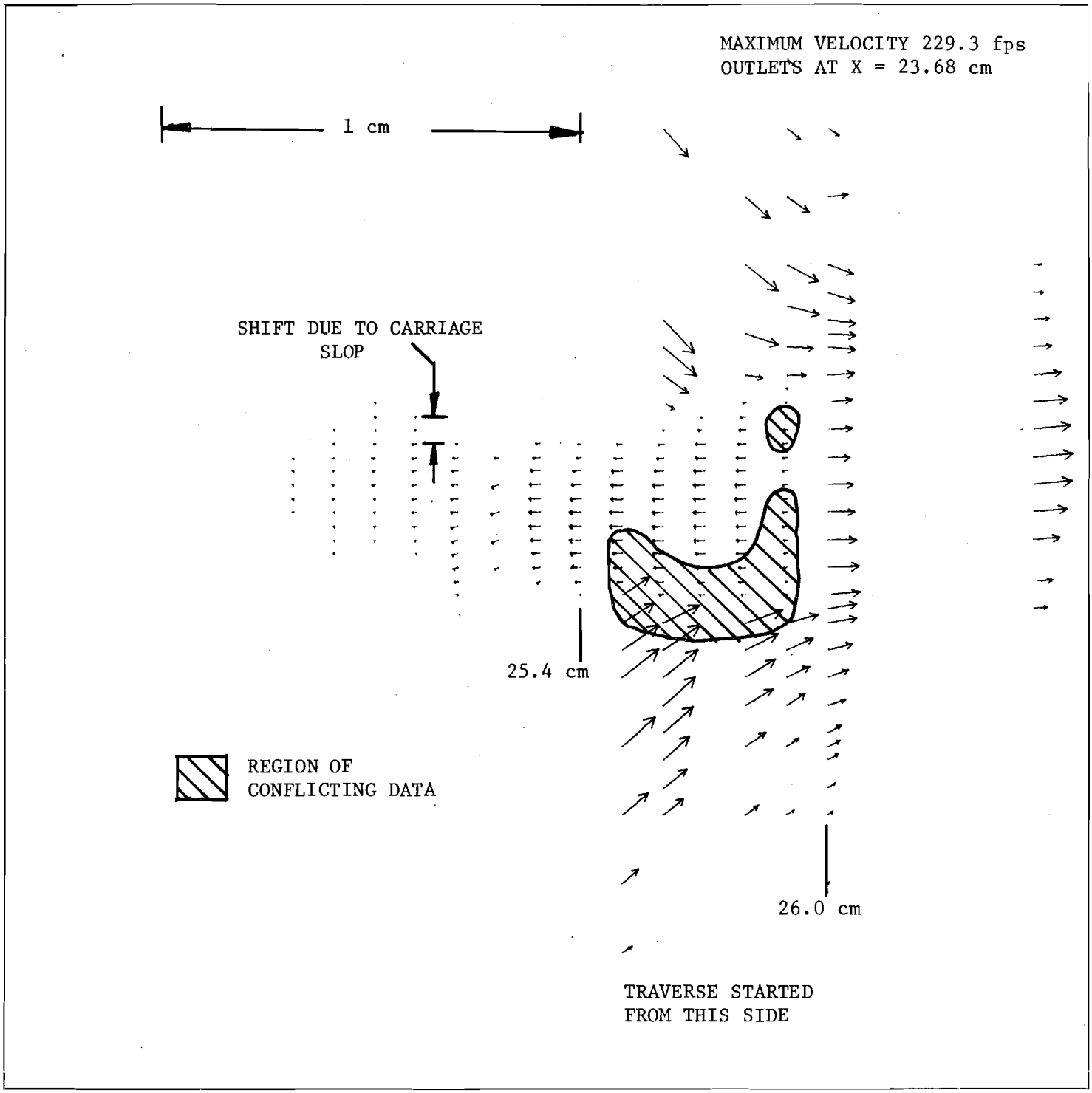

Fig. 3. Velocity vectors in the plane of the jets.

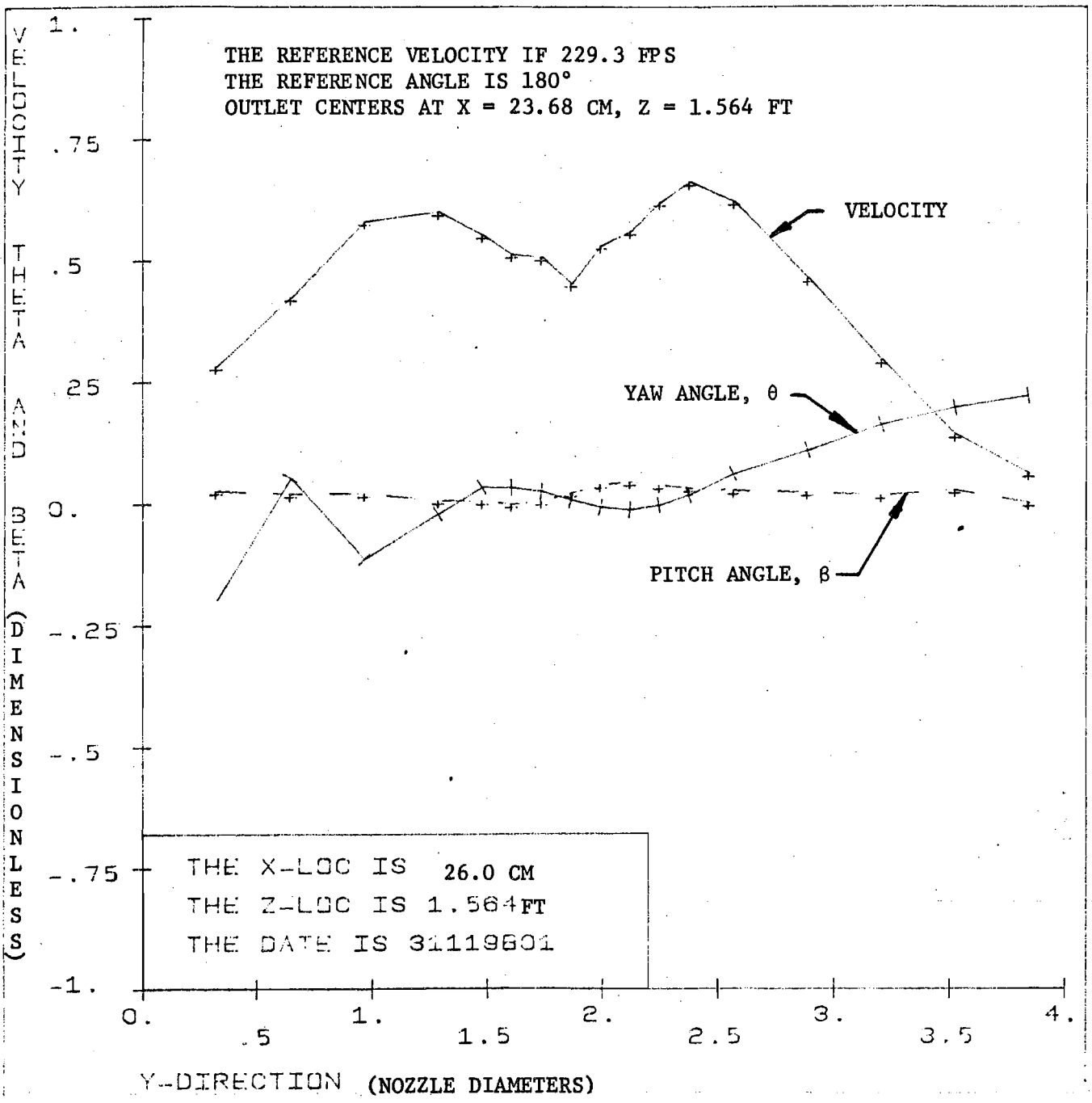

Fig. 4. Velocity in the forward flow in the plane of the nozzles.

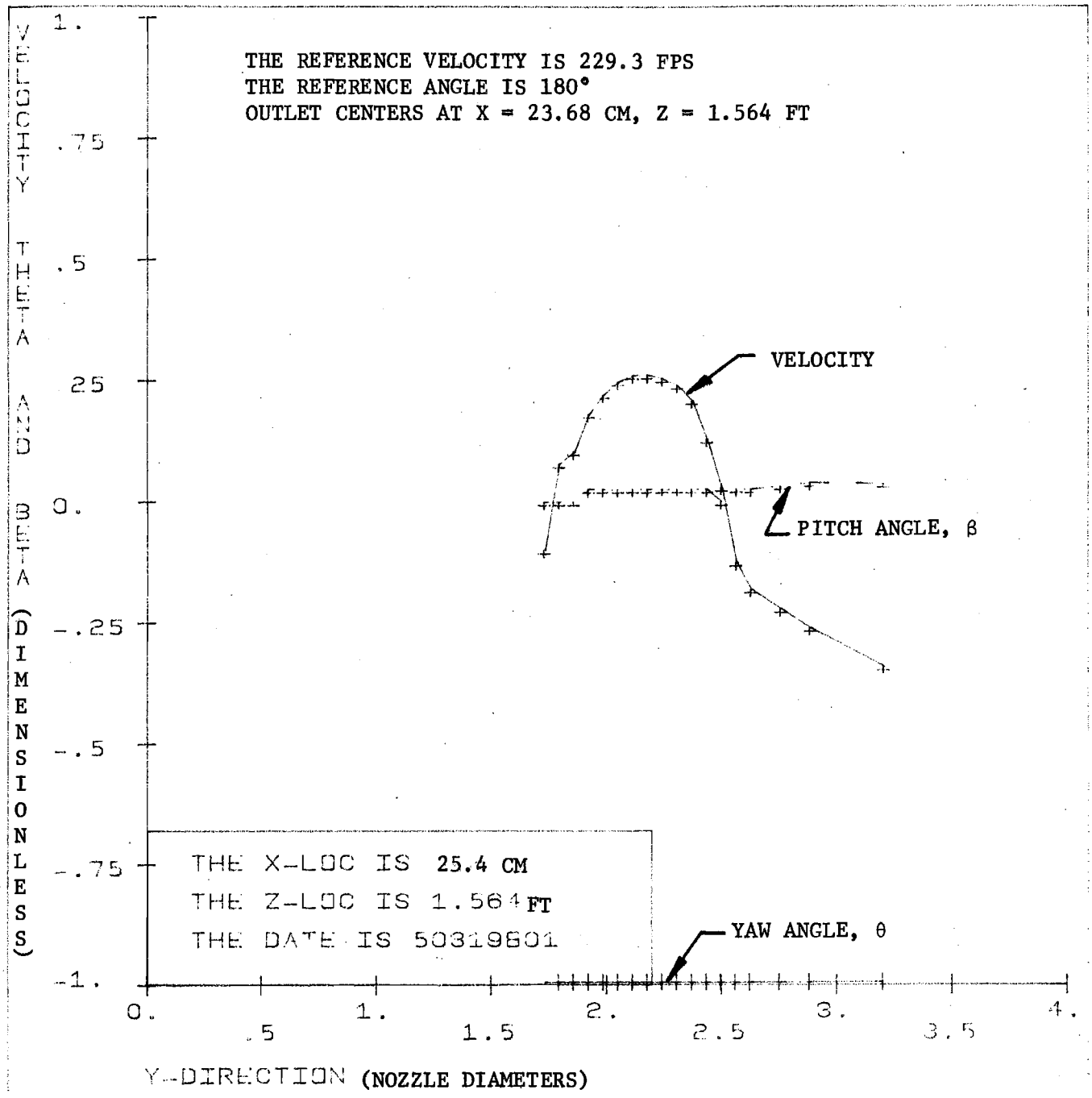

Fig. 5. Velocity traverse in the backflow in the plane of the nozzles.

angle and pitch angle in the forward flow region as the two incoming jets merge. Its general form suggests the conjunction of two essentially Gaussian profiles. Figure 5, on the other hand, shows the same parameters in the region of backflow. Clearly the velocity profile in that region is non-Gaussian in character.

Figs. 6 through 9 show contours of equal velocity at four locations in the flow field. Figs. 6 through 8 are located in the region of backflow. These illustrate that the backflow spreads much more rapidly in the z-direction than in the y-direction. Fig. 9 is in the forward flow. Note that it is plotted to a different linear scale than the three preceding figures. Figs. 10 through 13 show three dimensional surface projections of the same data viewed from a point on a line parallel to the x-axis, with the line of sight depressed 15° towards the yz plane and at an angle of 45° to both the x and y directions.

In order to create Figs. 6 through 13 matrices were formed to hold data from traverses taken at intervals of z. Since the z intervals were less in some flow regions than others, intermediate profiles were created by linear interpolation where data did not exist. Then, to correct for that fact that units and intervals of measurements were different in the y and z directions,a new matrix was created using a four point interpolation scheme. This latter matrix is that upon which the plots are based. The elements of the matrix are thus not necessarily physical data, but artificial data created by interpolation.

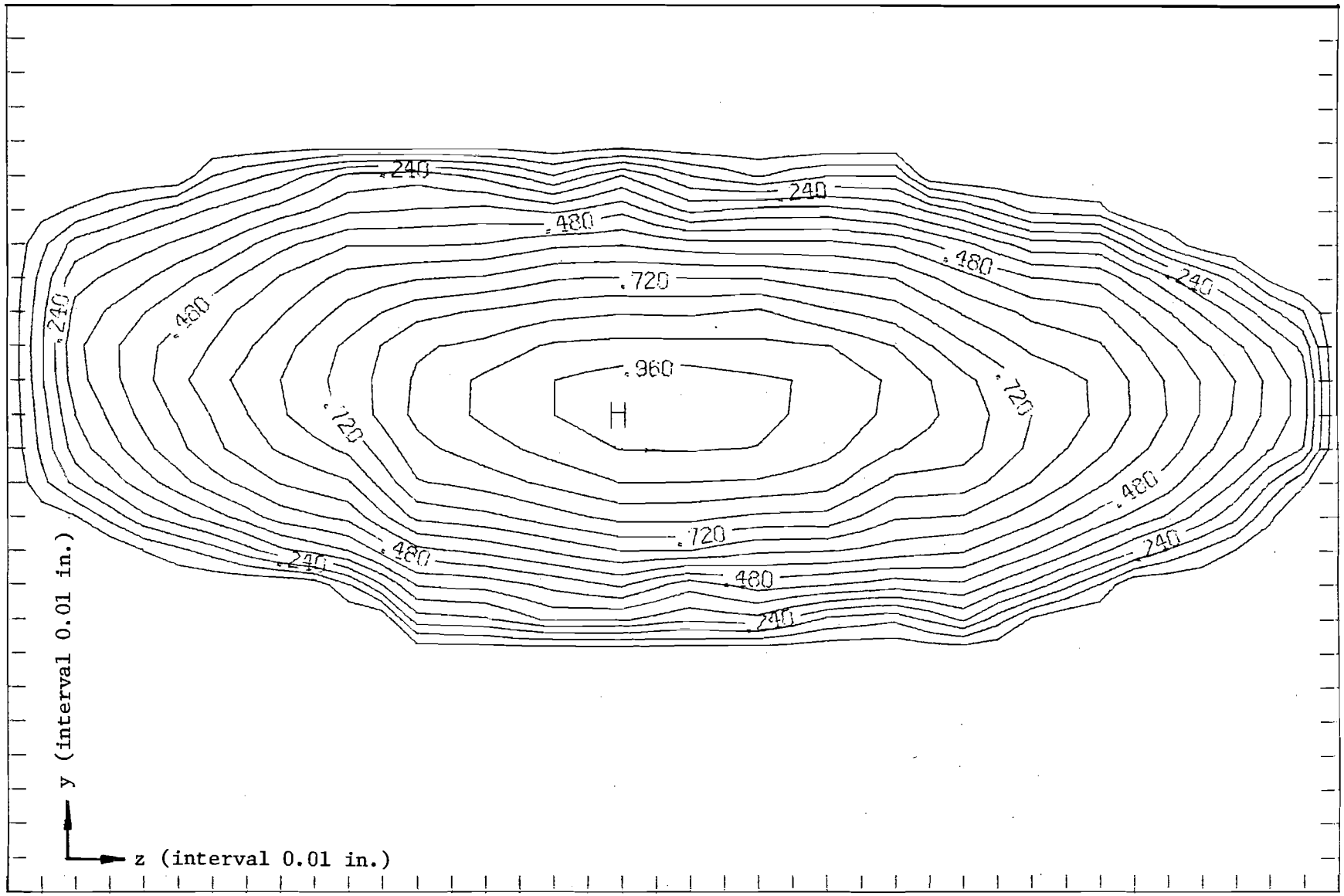

Fig. 6. Contours of equal velocity in the backflow at x = 25.2 cm

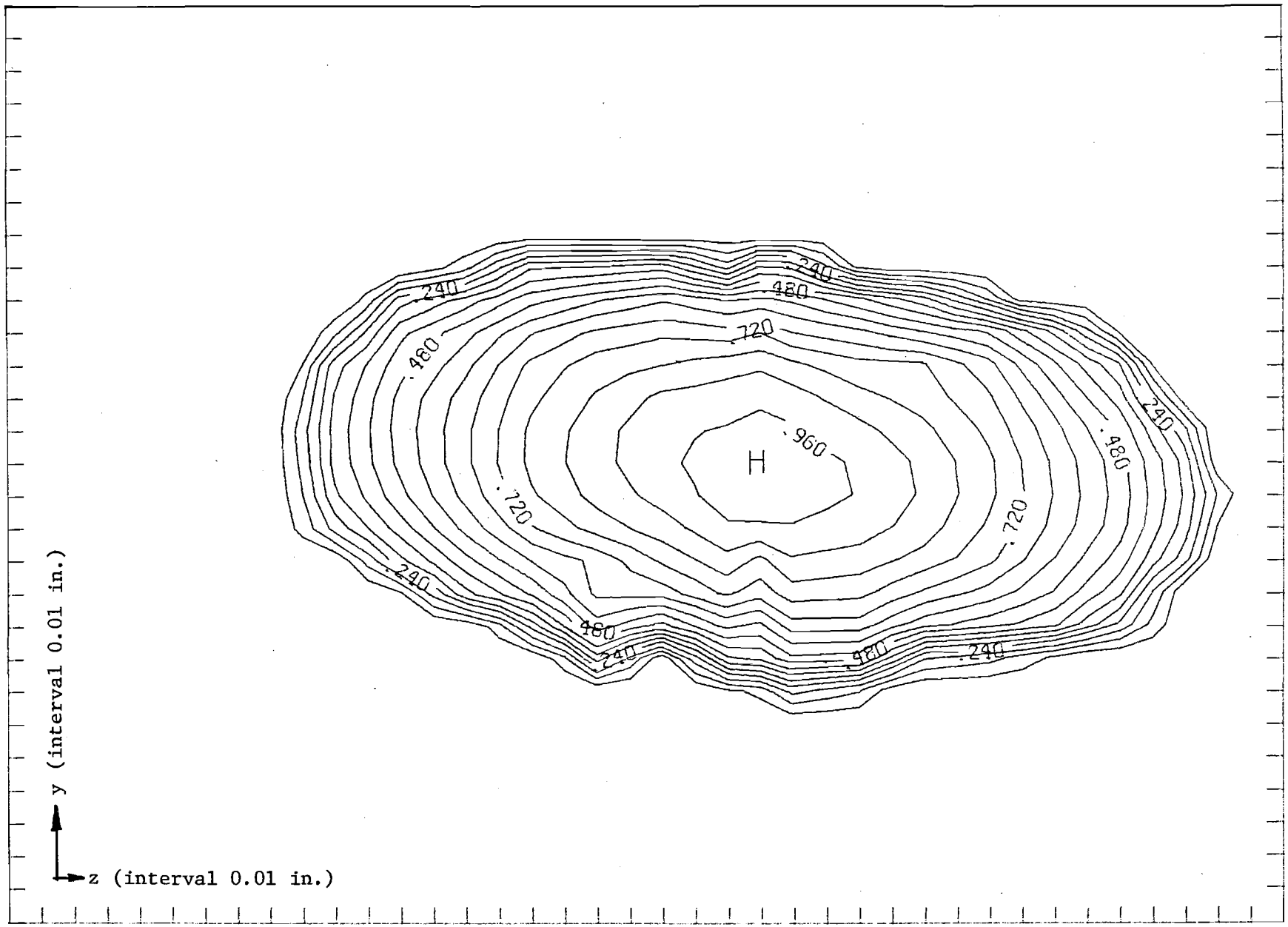

Fig. 7. Contours of equal velocity in the backflow at x = 25.5 cm.

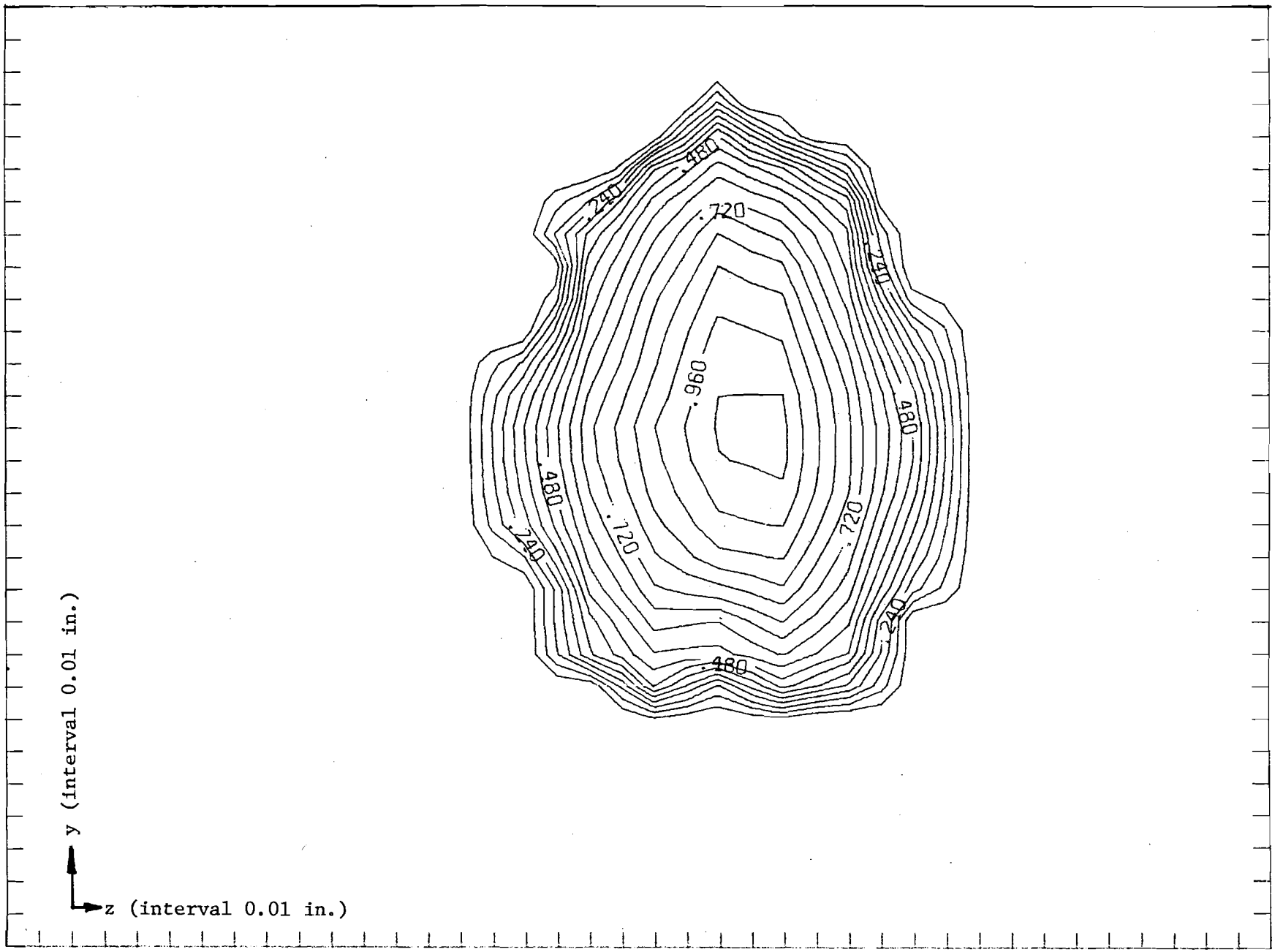

Fig. 8. Contours of equal velocity in the backflow at x = 25.8 cm.

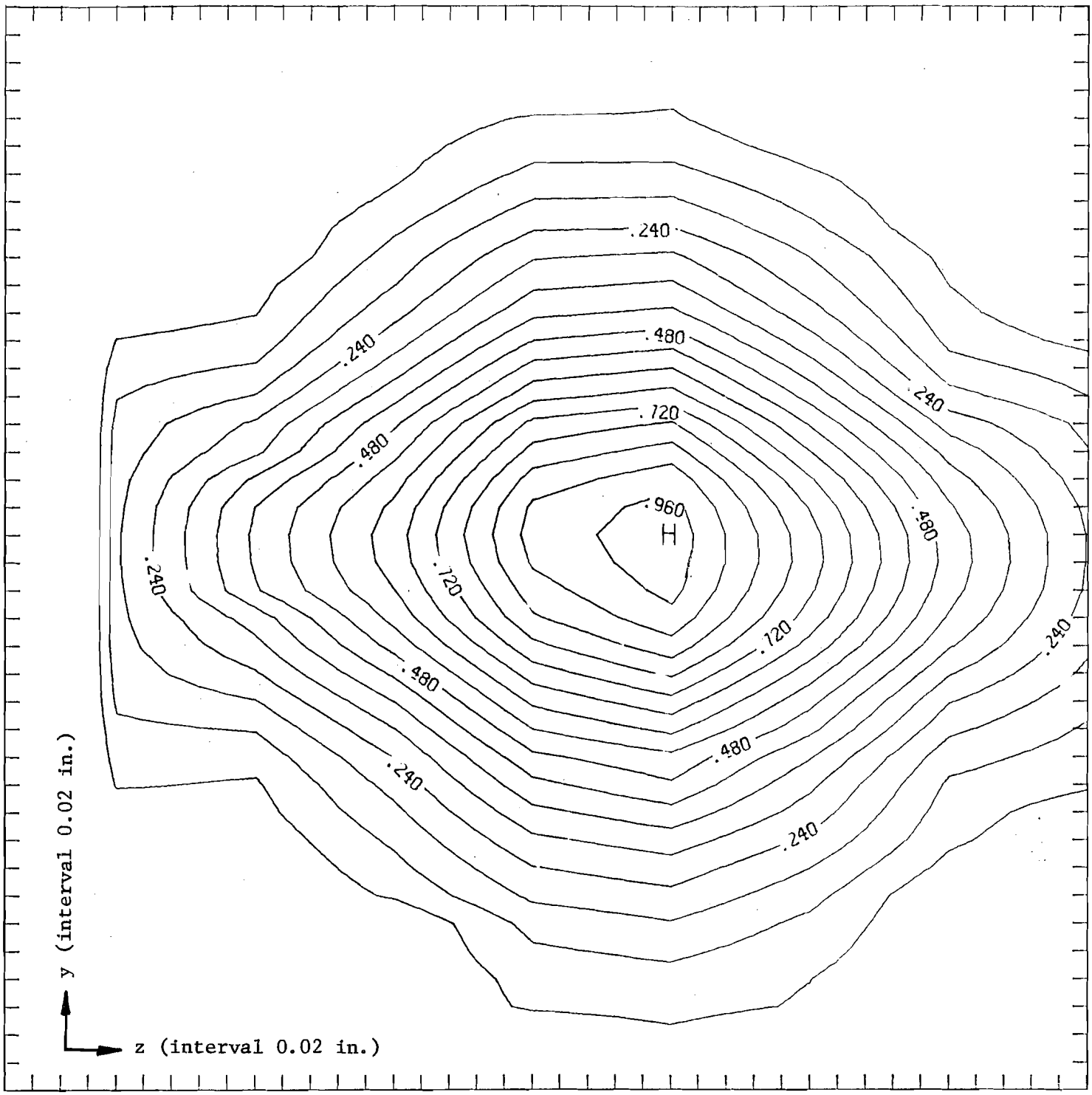

Fig. 9. Contours of equal velocity in forward flow at x = 26.2 cm.

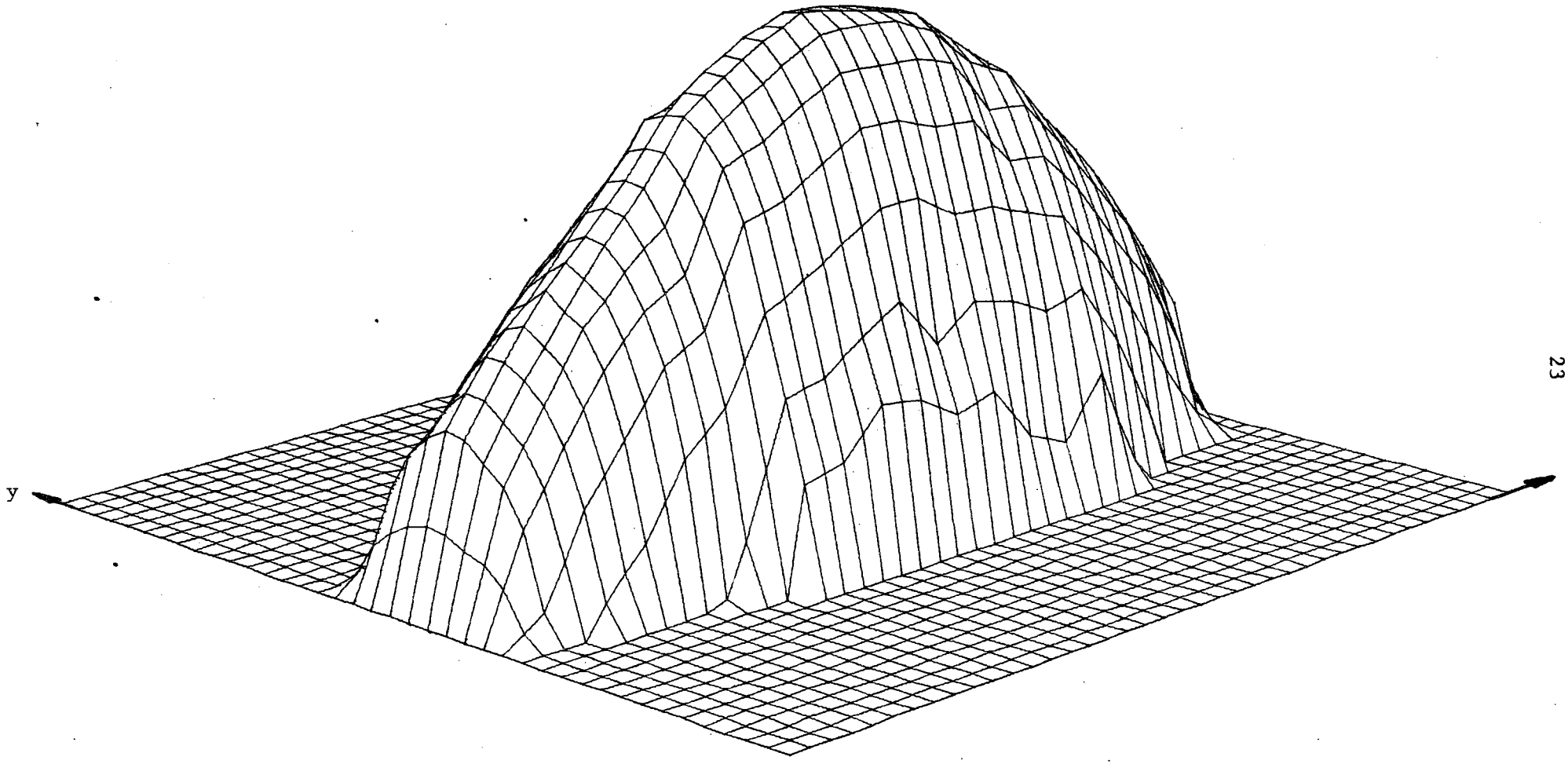

Fig. 10. Isometric projection of surface representing backflow velocities at x = 25.2 cm.

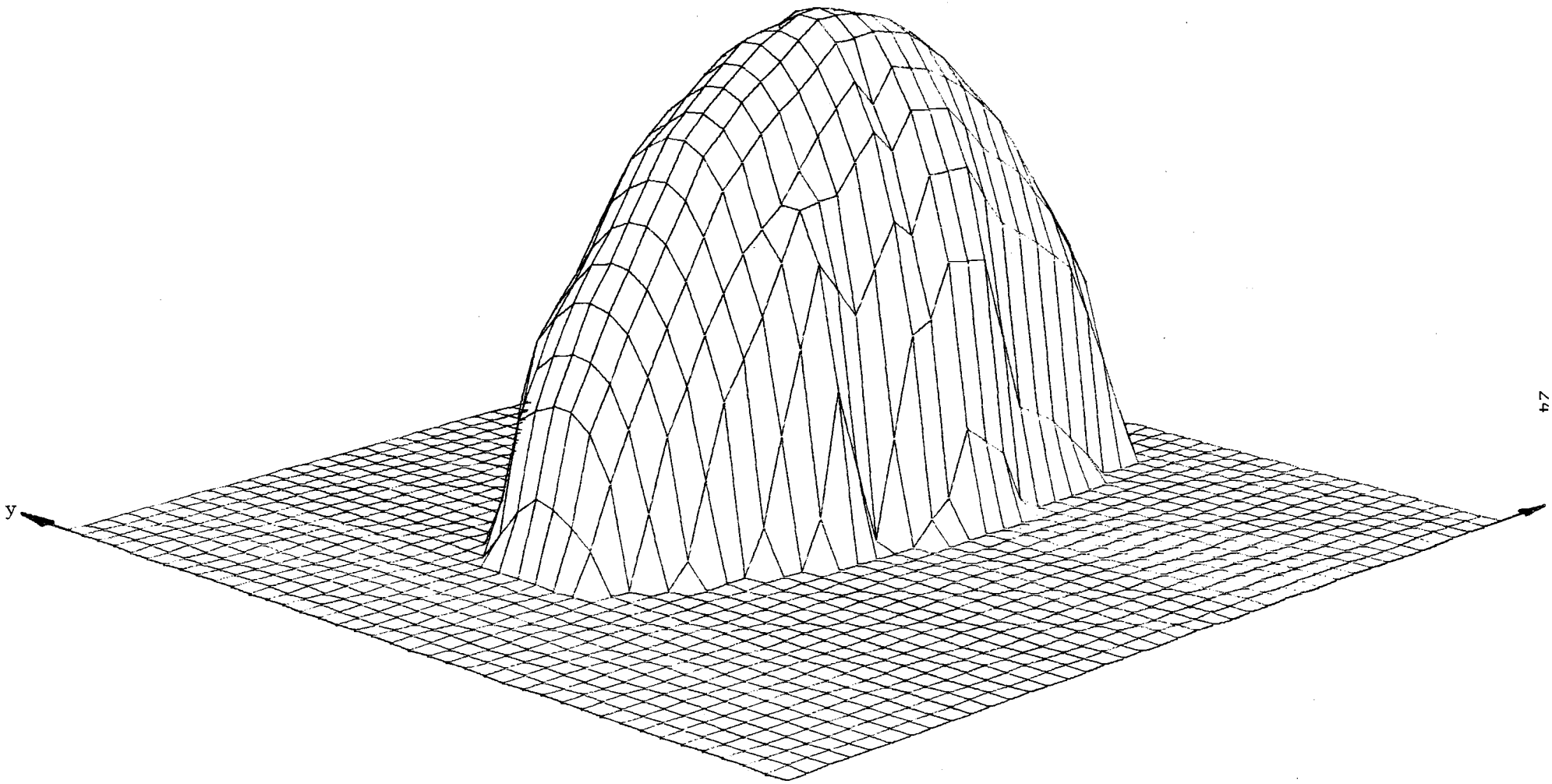

Fig. 11. Isometric projection of surface representing backflow velocities at x = 25.5 cm.

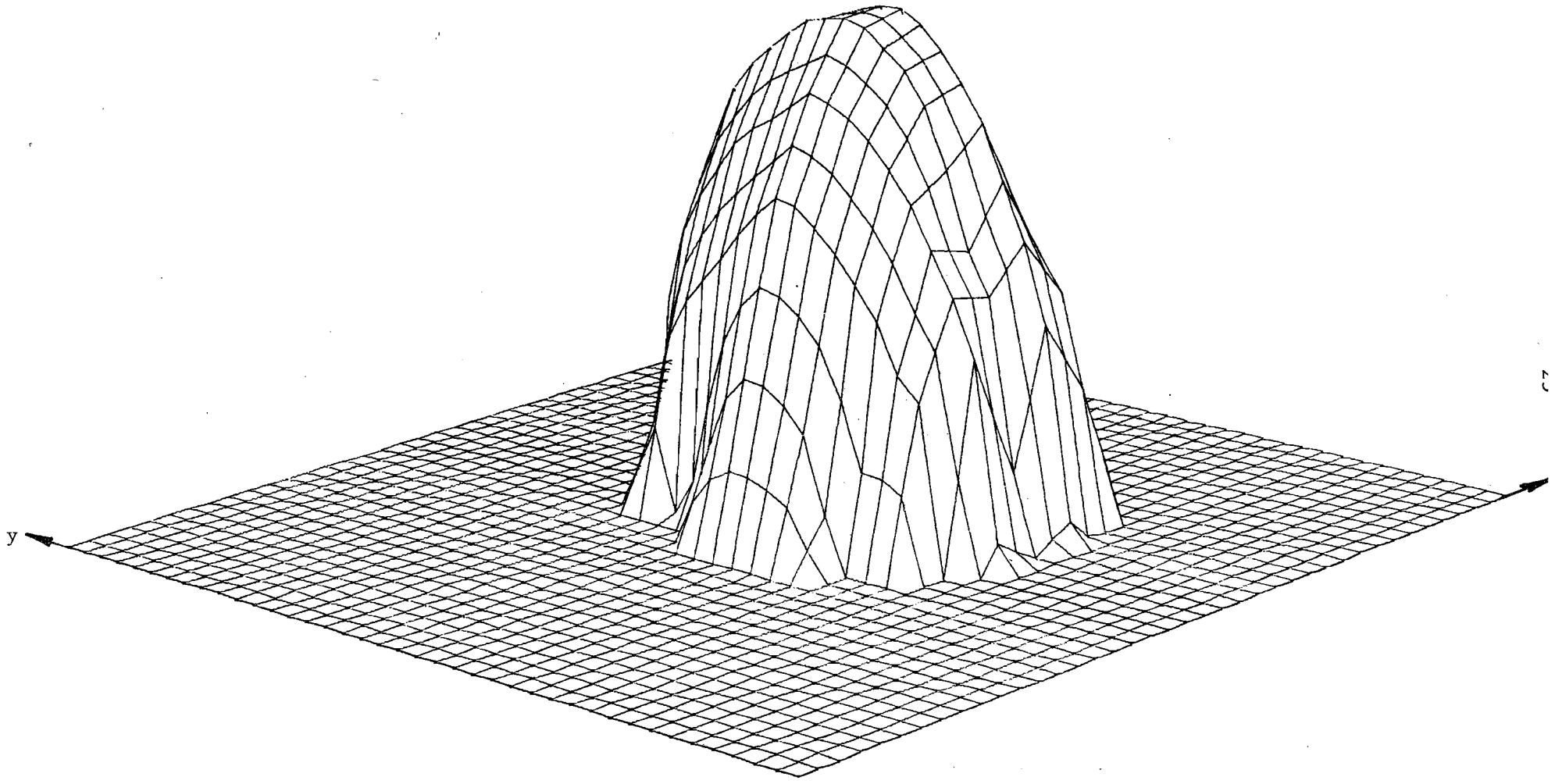

Fig. 12. Isometric projection of surface representing velocities at x = 25.8 cm.

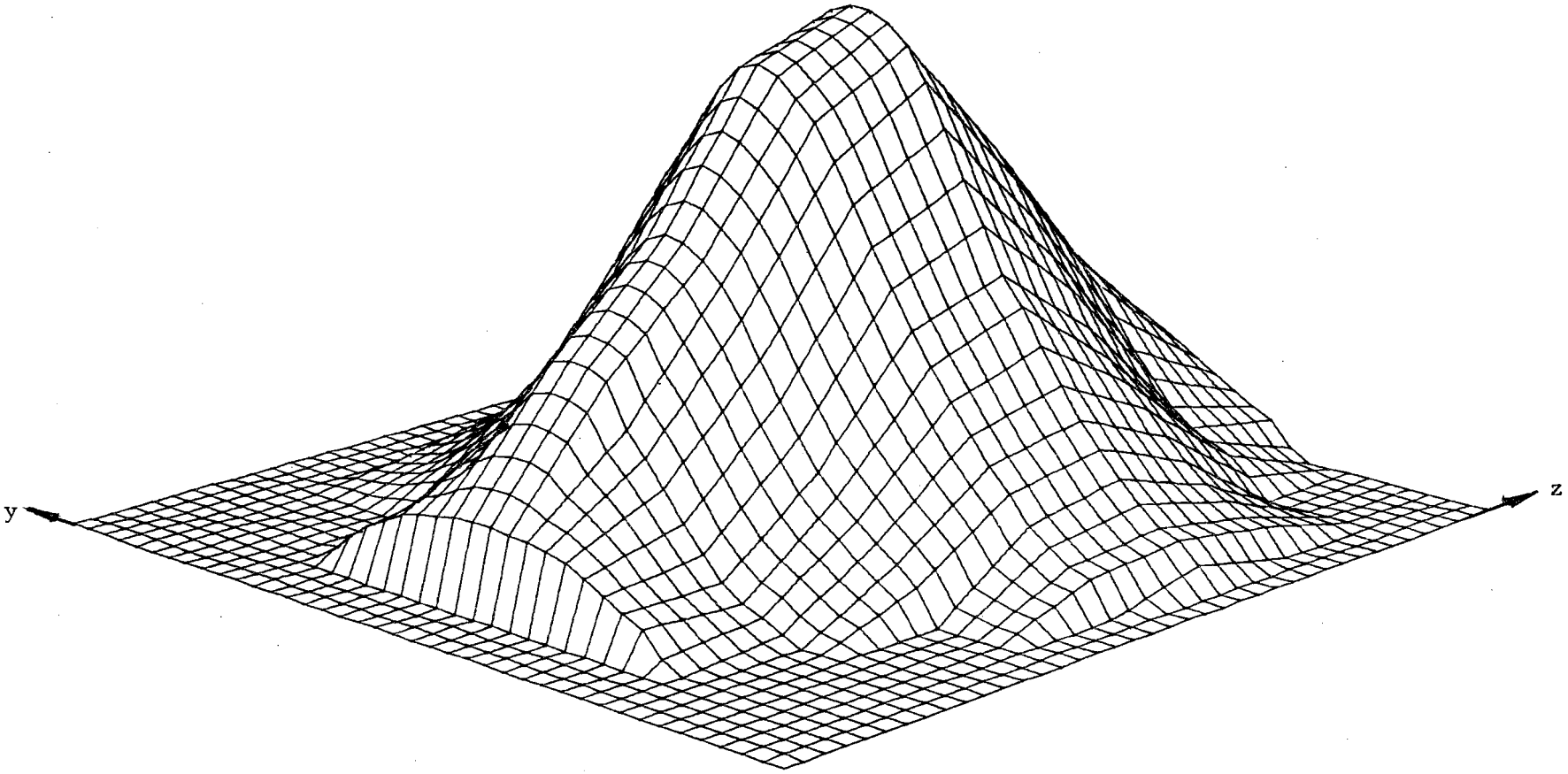

Fig. 13. Isometric projection of surface representing forward velocities at x = 26.2 cm.

4. DATA ANALYSIS

In order to develop assumptions as to the character of similarity profiles in the flow, which could be used as the basis for development of a solution, the forward and backward flow profiles were examined for similarity.

Figure 14 shows the profiles measured in the forward flow compared with a normal distribution. Clearly they are essentially Gaussian in character. Figure 15, on the other hand, shows the velocity profiles in the plane of the nozzle in the back flow. Since there is reversal of flow at the edge of the jet, the jet width for zero velocity may be clearly defined. However, since in most circumstances such a distinct profile edge does not exist, it has become customary to work with the half-width of the velocity profile, i.e. the width of the profile when the velocity is equal to half the maximum value. In this case b_y = half-width in the xy plane and b_z = half-width in the xz plane. Because there is a distinct edge to the jet a Gaussian profile would not be appropriate. Figure 15 has plotted on it a cubic curve and an ellipse as possible simple functions. The ellipse fits the data well in the region of higher velocities and less well in the region where velocities are less reliable. It is of course possible to alter the abscissa scale to make the dimensionless base width of the profile equal to one, in which case the semi-ellipse becomes a semi-circle. The equation for the ellipse is

$$u/u_m = [1 - 3\ (\Delta y/b_y)^2]^{1/2} \tag{3}$$

The cubic equation is given by

$$u/u_m = 1 - 0.30\ (\Delta y/b_y) + 0.29\ (\Delta y/b_y)^2 - 3.37\ (\Delta y/b_y)^3 \tag{4}$$

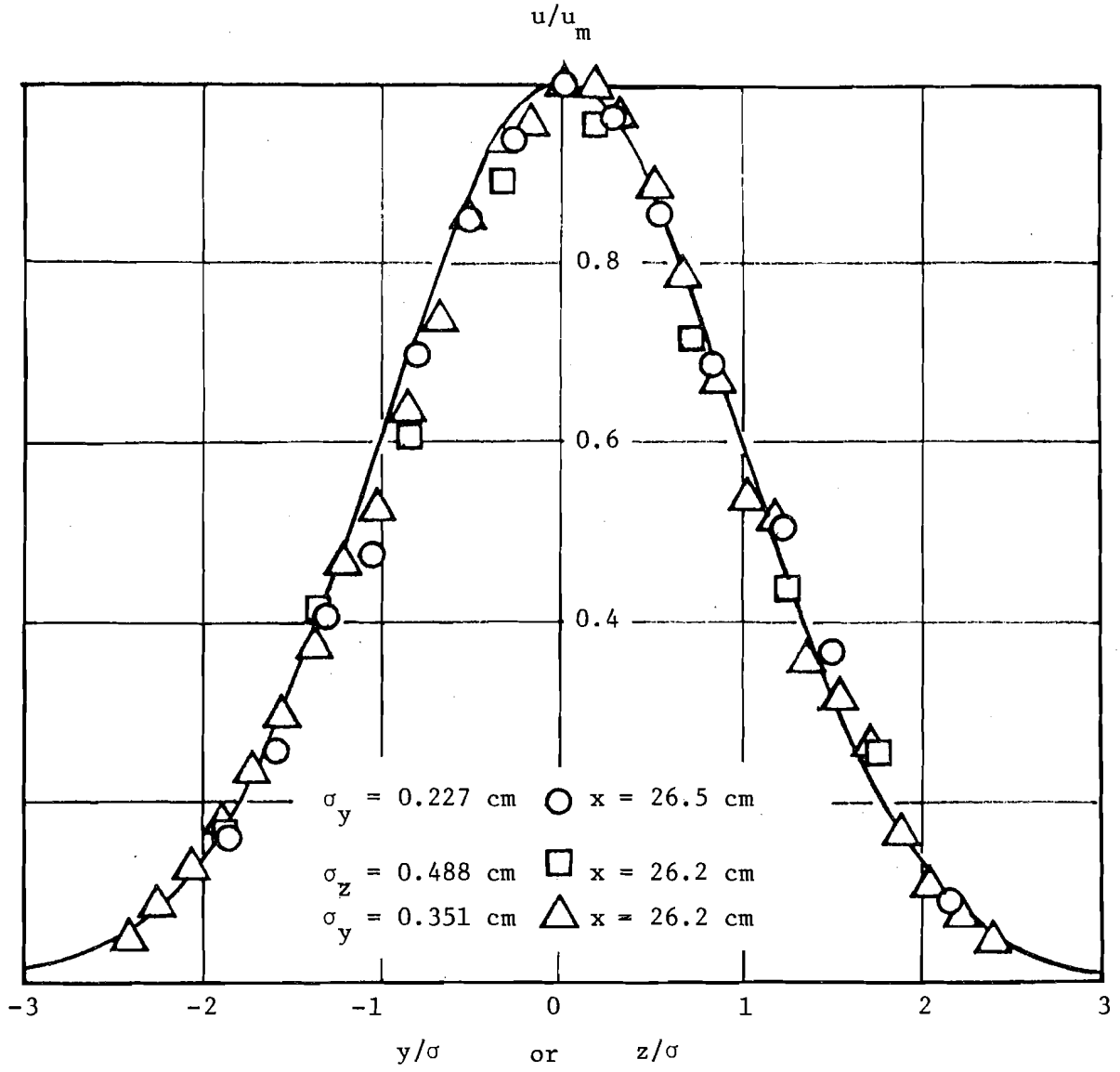

Fig. 14 Forward flow profiles compared with Gaussian distribution

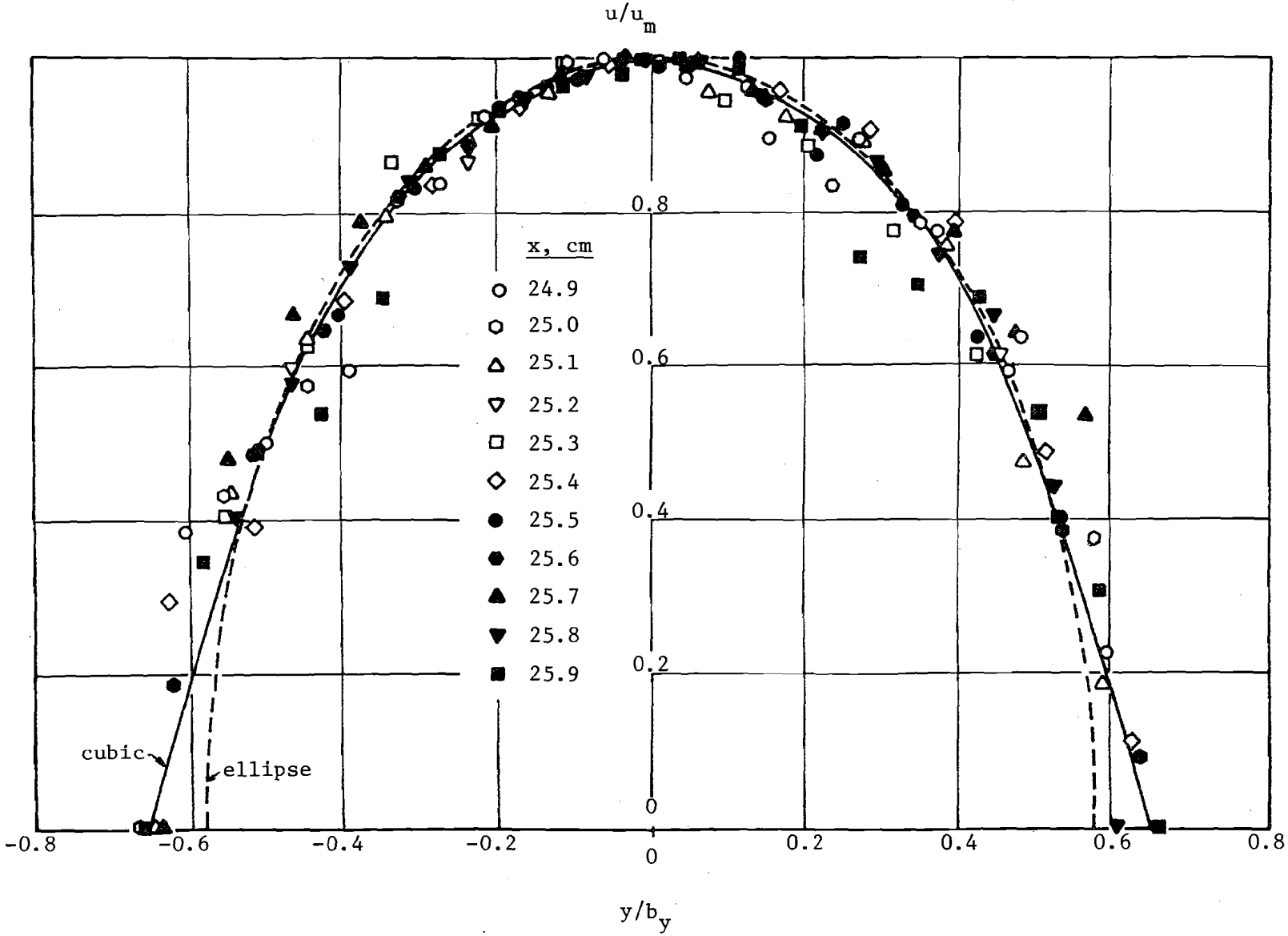

Fig. 15 Velocity profiles in the plane of the nozzles in the backflow

Figure 16 shows the corresponding plot for the vertical distribution of velocities in the back flow. In this case the data is well fit by a simple cosine function

$$u/u_m = \cos\left(\frac{2\pi}{3}\ \frac{\Delta z}{b_z}\right) \tag{5}$$

Since there is no clear reversal of direction at the upper and lower edges of this profile it may also be quite well fit by the Gaussian distribution

$$u/u_m = \exp\left[-2.77\ (\Delta z/b_z)^2\right] \tag{6}$$

Thus, the profile in the reverse flow may be represented by a combination of Eq. 3 or 4 with Eq. 5 or 6.

Figure 17 shows the measured values of b_y and b_z in the reverse flow, and the observed values of σ in the forward flow.

The stagnation point obtained by linear interpolation from the profiles shown on Fig. 3, is indicated on Fig. 17 for reference. The data suggests that, after some initial distance back from the stagnation point, there is negligible spreading in the plane of the nozzles and approximately linear spreading normal to this plane.

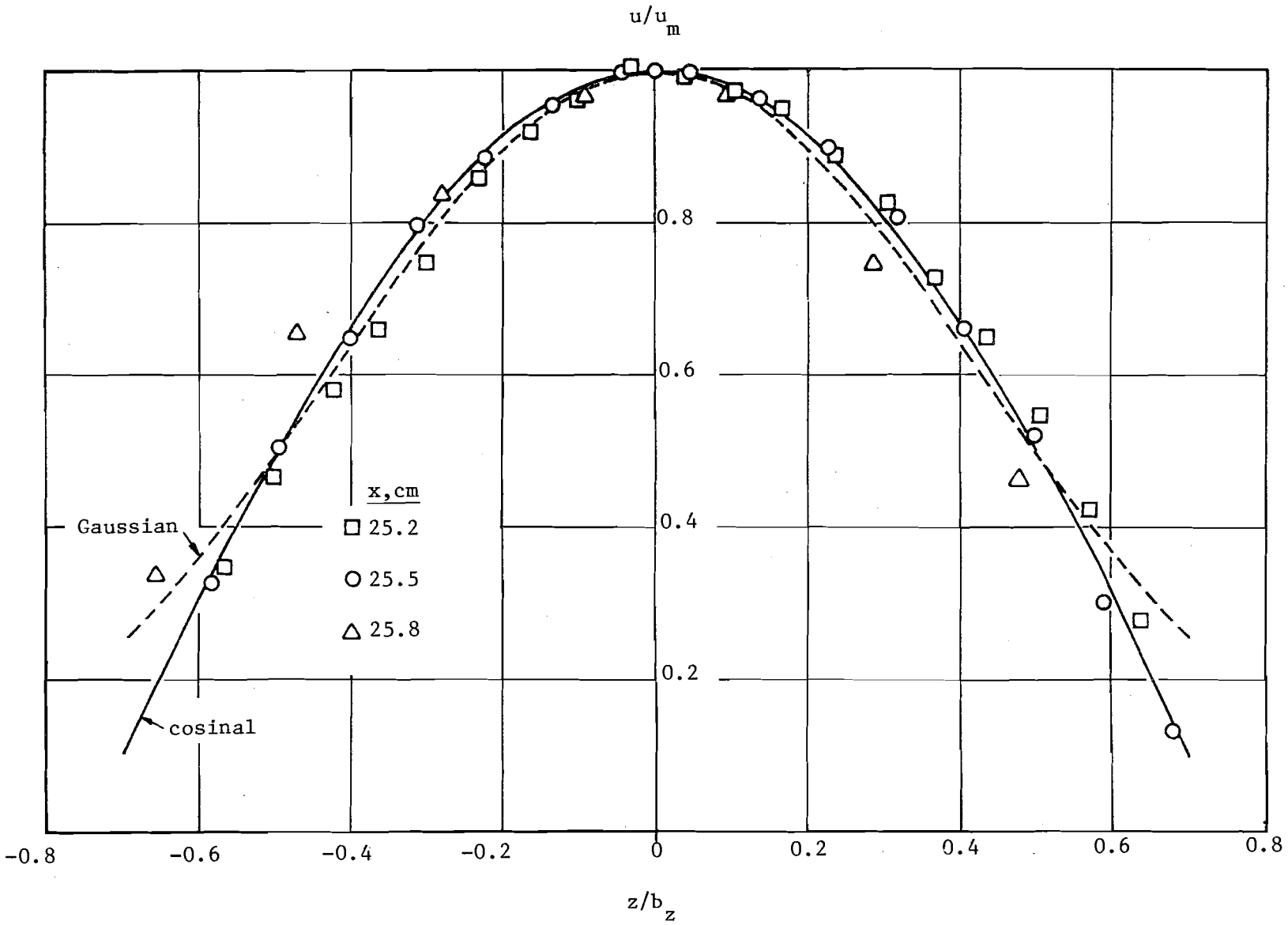

Fig. 16 Velocity profiles normal to the plane of the nozzles in the backflow

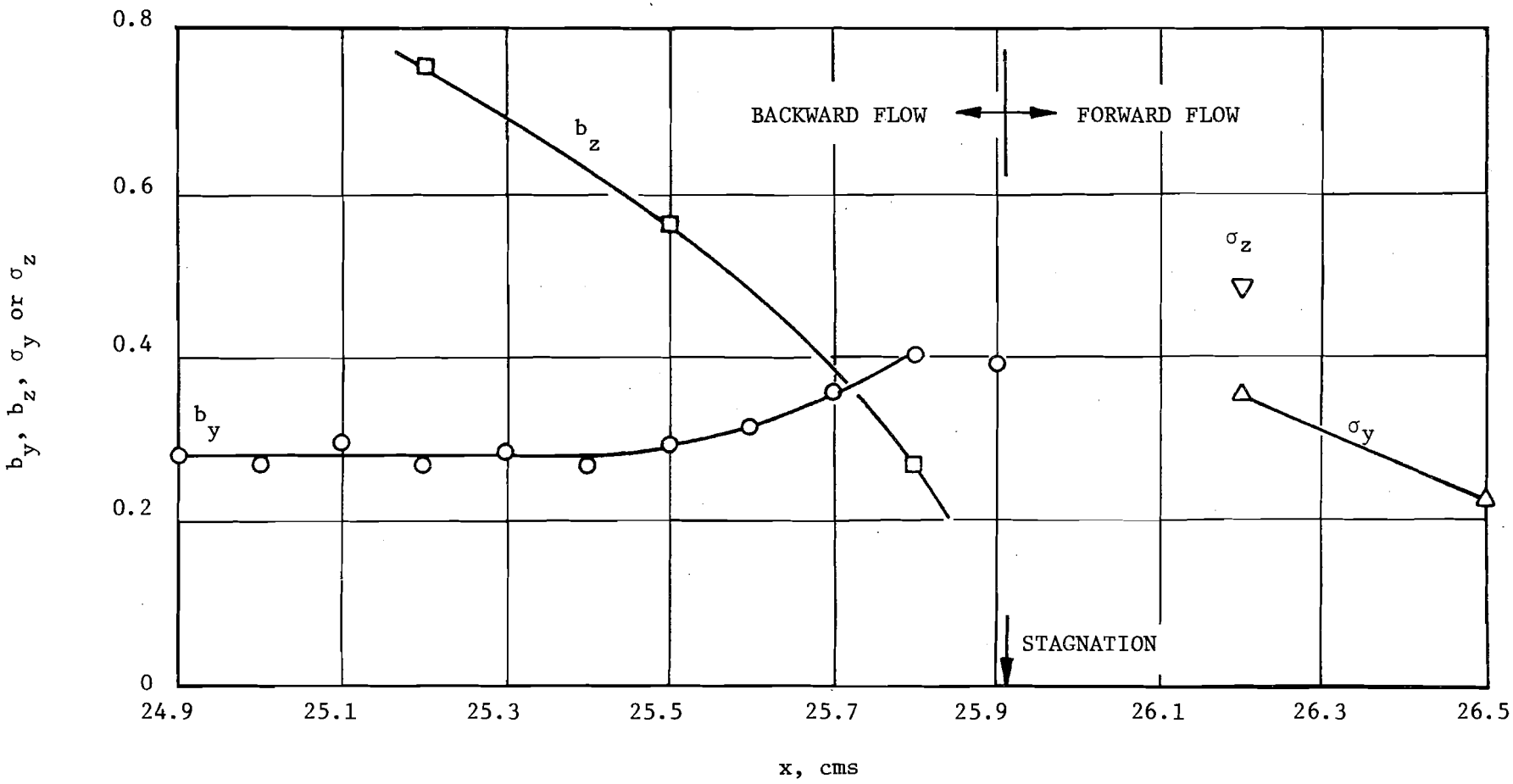

Fig. 17 Profile widths in the forward and backflows

5. CONCLUSIONS AND RECOMMENDATIONS

5.1. Conclusions

Intersecting flow may not necessarily be combined using vector addition of velocities or momentum flux densities. When two perpendicular intersecting axisymmetric submerged turbulent jet flows of approximately equal strength combine, a region of backflow is observed. The backflow spreads much more rapidly in the direction perpendicular to the plane of the nozzles than it does in the plane of the nozzles. In the region of forward flow the profiles were essentially Gaussian. In the region of backflow the profiles were approximately elliptic or cubic in the plane of the nozzle, and approximately Gaussian or cosinal normal to this plane. After some initial distance back from the stagnation point observed in the flow, spreading in the backflow in the plane of the nozzles appeared to be negligible and approximately linear normal to this plane. Attempts to develop an analytic solution for the flow field have so far proved unsuccessful. The similarity profiles may, however, provide the basis for useful assumptions in developing such a solution. Because of the limited amount of data which could be collected in this investigation, it would be unwise to attempt to draw any general conclusions about the magnitudes of empirical coefficients used to fit mathematical formulations to the observed data.

5.2. Recommendations on Future Applications

The work described in this report represents an initial investigation of a phenomenon that, when more fully understood, can lead to an improvement in the quality of predictive computational models for the flow fields involving zones of chemical, sedimentary or thermally altered discharges into moving currents. Present methods are generally based on the notion that an accurate general description of the flow field may result from vector combinations of

velocities or momentum fluxes on an elementary level. Such models then have to be modified to take into account wake effects by the introduction of drag coefficients. Extension of the present work which might lead to improved modeling of the elementary process used to synthesize the overall flow pattern would include numerical analytic investigation of the pressure field that develops when a simple jet is directed at an angle toward a flat surface, and the extension of this investigation to the pressure field within the flow created by two merging streams. Finally, a theoretical basis should be sought to justify the combination of small elements of large flow fields, taking into account backflows (which may be overridden by the forward flow in a proximate element). This would provide the possibility of predicting a flow pattern involving backflows in some regions without the necessity of introducing artificial concepts such as drag coefficients accounting for the blockage effect of the injected flow.

LIST OF REFERENCES

1. Abraham, G., "Jet Diffusion in Stagnant Ambient Fluid," Delft Hydraulics Laboratory Publications, No. 29, July, 1963.

2. Albertson, M. L., Dia, Y. B., Jensen, R. A., and Rouse, H., "Diffusion of Submerged Jets," Transactions, ASCE, Vol. 115, Paper No. 2409, 1950 pp. 639-697.

3. Alexander, L. G., Baron, T., and Comings, E. W., "Transportation of Momentum, Mass, and Heat in Turbulent Jets," Bulletin Series No. 413, University of Illinois Engineering Experiment Station, Urbana, Ill., May, 1953.

4. Becher, P., "Luftstrahlen aus Ventilations-öffnungen, Gesundheits ingenieur, No. 9/10, Mai, 1950, pp. 139-145.

5. Betz, A., "Versuche über die Ausbreitung eines freien Strahles," Ergebnisse der Aerodynamischen Versuchsanstalt zu Göttingen, II, 1923. pp. 69-73.

6. Bradbury, L.J.S., "An Investigation Into the Structure of a Turbulent Plane Jet," Ph.D. Thesis, University of London, 1963.

7. Corrsin, S., "Investigation of Flow in an Axially Symmetrical Jet of Air," N.A.C.A. Wartime Reports, W-94, Dec., 1943.

8. Corrsin, S., and Uberoi, M. S., "Further Experiments on the Flow and Heat Transfer in Heated Turbulent Air Jet," N.A.C.A. Technical Notes, N 1865, April, 1949.

9. Corrsin, S., and Uberoi, M. S., "Further Experiments on the Flow and Heat Transfer in a Heated Turbulent Air Jet., N.A.C.A. Reports, No. 998, 1950.

10. Fischer, H. B., List, E. J., Koh, R.C.Y., Imberger, J., and Brooks, N.H., Mixing in Inland and Coastal Waters, Academic Press, New York, N.Y., 1979.

11. Flora, J., and Goldschmidt, V., "Virtual Origins of a Free Plane Turbulent Jet," American Institute of Aeronautics and Astronautics Journal, Vol. 7, 1969, pp. 2344-2346.

12. Forstall, W., and Gaylord, E. W., "Momentum and Mass Transfer in a Submerged Water Jet," Journal of Applied Mechanics, Vol. 22, 1955, pp. 161-164.

13. Förthmann, E., "Turbulent Jet Expansion," N.A.C.A. Technical Memoranda, No. 789: Translated from Ing. Arch., Vol. 5, 1934, pp. 42-54.

14. Gartshore, I. S., "The Streamwise Development of Two-Dimensional Wall Jets and Other Two-Dimensional Turbulent Shear Flows," Ph.D. Thesis, Mechanical Engineering, McGill University, 1965.

15. Goldschmidt, V., and Eskinazi, S., "Two Phase Turbulent Flow in a Plane Jet," Journal of Applied Mechanics, Vol. 33, 1966, pp. 735-747.

16. Hegge Zijnen, B. G. van der, "Measurements of the Velocity Distribution in a Plane Turbulent Jet of Air," Applied Scientific Research, Vol. 7, Section A, 1958, pp. 256-276.

17. Heskestad, G., "Two Turbulent Shear Flows," Johns Hopkins University, Mechanical Engineering Contract AF(638)-248, 1963.

18. Heskestad, G.,"Hot Wire Measurements in a Plane Turbulent Jet," Journal of Applied Mechanics, Vol. 32, 1965, pp. 721-734 (erratum, Sept. 1966, p. 710).

19. Hinze, J. O., and Hegge Zijnen, B. G. van der, "Transfer of Heat and Matter in the Turbulent Mixing Zone of an Axially Symmetric Jet," Applied Scientific Research, The Hague, Section A, Vol. 1, 1949, pp. 435-461.

20. Jenkins, P. E., and Goldschmidt, V., "Mean Temperature and Velocity in a Plane Turbulent Jet," Journal of Fluids Engineering, Transactions ASME, Vol. 95, 1973, pp. 581-584.

21. Johannesen, N. H., "Further Results on the Mixing of Free Axially-Symmetrical Jets of Mach Number 1.40," Aeronautical Research Council Technical Report, R and M No. 3292, 1962.

22. Keagy, W. R., and Weller, A. E., "A Study of Freely Expanding Inhomogeneous Jets," Heat Transfer Fluid Mechanics Institute, 2nd Berkeley, California, 1949, pp. 89-98.

23. Keagy, W. R., Weller, A. E., Reed, F. A., and Reid, W. T., Batelle Memorial Institute, The Rand Corporation, Santa Monica, California, Feb., 1949.

24. Kizer, K. M., "Material and Momentum Transport in Axisymmetric Turbulent Jets of Water," American Institute of Chemical Engineers Journal, Vol. 9, 1963, pp. 386-390.

25. Knystautas, R., "The Turbulent Jet From a Series of Holes in Line," Aeronautical Quarterly, Vol. 15, 1964, pp. 1-28.

26. Kotsovinos, N. W., "A Study of the Entrainment and Turbulence in a Plane Turbulent Jet," W. M. Keck Laboratory Reports, KH-R-32 California Institute of Technology, Pasadena, California, 1975.

27. Kotsovinos, N. E., "A Note on the Spreading Rate and Virtual Origin of a Plane Turbulent Jet," Journal of Fluid Mechanics, Vol. 77, Part 2, 1976, pp. 305-311.

28. Maxwell, W. H. C., and Snorrason, A., "Measurements in Intersecting Submerged and Induced Jets," University of Illinois Civil Engineering Studies, Hydraulic Engineering Research Series, No. 34, Aug. 1979.

29. Maxwell, W. H. C., "Crossing Submerged Jets," Journal of the Hydraulics Division, ASCE, Vol. 105, No. HY12, Proc. Paper 15016, Dec. 1979, pp. 1557-1560.

30. Mih, W. C., and Hoopes, J. A., "Mean and Turbulent Velocities for Plane Jet," Journal of Hydraulics Division, ASCE, Vol. 98, 1972, pp. 1274-1294.

31. Miller, D. R., and Comings, E. W., "Static Pressure Distribution in the Free Turbulent Jet," Journal of Fluid Mechanics, Vol. 3, Part I, 1957, pp. 1-16.

32. Nakaguchi, H., "Jet Along a Curved Wall," University of Tokyo Research Memoranda, No. 4, 1961.

33. Newman, B. G., "Turbulent Jets and Wakes in a Pressure Gradient," Fluid Mechanics of Internal Flow, G. Sovran, ed., Elsevier Publishing Company, The Netherlands, 1967, pp. 170-209.

34. Olson, R. E., "An Analytical and Experimental Study of Two-Dimensional Submerged Jets," Diamond Ordnance Labs., Proceedings of the Fluid Amplification Symposium, 1962, pp. 267-286.

35. Poreh, M., and Cermak, J. E., "Flow Characteristics of a Circular Submerged Jet Impinging Normally on a Smooth Boundary," Sixth Mid-Western Conference on Fluid Mechanics, University of Texas, 1959, pp. 198-212.

36. Reichardt, H., "Gesetzmäszigkeiten der freien Turbulenz," V.D.I. Forschungsheft, Vol. 13, May-June, 1942, pp. 1-22.

37. Reichardt, H., "Gesetzmassigkeiten der Freien Turbulenz," V.D.I. Forschungsheft, Vol. 414, 1951.

38. Ricou, F. P., and Spalding, D. R.,"Measurements of Entrainment by Axisymmetrical Turbulent Jets," Journal of Fluid Mechanics, Vol. 11, 1961, pp. 21-32.

39. Rosenweig, R. E., Hottel, H. C., and Williams, C. G., "Smoke Scattered Light Measurement of Turbulent Concentration Fluctuations," Chemical Engineering Science, Vol. 15, 1961, pp. 111-129.

40. Ruden, P., "Turbulente Ausbneitrorgönge im Freistahl," Naturwissenschaften, Vol. 21, 1933, pp. 375-378.

41. Taylor, J. F., Grimmett, H. L., and Comings, E. W., "Isothermal Free Jets of Air Mixing with Air," Chemical Engineering Progress, Vol. 47, No. 4, April, 1951, pp. 175-180.

42. Trüpel, T., "Uber die Einwirkung eines Luftstrahles auf die umgebende Luft," Zeitschrift für das gesamte Turbinenwesen, Vol. 12, No. 5, 1915, pp. 52-66.

43. Uberoi, M., and Garby, L. C., "Effect of Density Gradient on an Air Jet," Physics of Fluids, Vol. 10, 1967, pp. 200-202.

44. Wilson, R.A.M., and Danckwerts, P. V., "Studies in Turbulent Mixing .II. A Hot Air Jet," Chemical Engineering Science, Vol. 19, 1964, pp. 885-895.